

# Measuring Central Exclusive Processes at LHC

*Marek Taševský*

Institute of Physics, Academy of Sciences of the Czech republic, Na Slovance 2, 182 21 Prague, Czech republic

Diffractive physics program for experiments at the Large Hadron Collider is discussed with emphasis on measurements of central exclusive processes. At low luminosities, a L1 trigger based on requiring rapidity gaps can be used, while at high luminosities, the use of proton taggers proposed to be placed at 220 m and 420 m from the interaction point is foreseen.

## 1 Introduction

In this contribution, we focus on measurements of exclusive processes that could be performed at the multi-purpose LHC detectors, ATLAS and CMS. The central exclusive production (CEP) of new particles has received a great deal of attention in recent years (see [1] and references therein). The process is defined as  $pp \rightarrow p \oplus \phi \oplus p$  and all of the energy lost by the protons during the interaction (a few percent) is used in the production of the central system,  $\phi$ . The final state therefore consists of a centrally produced hard subprocess, two very forward protons and no other activity. The ' $\oplus$ ' sign denotes the regions devoid of activity, often called rapidity gaps. In Double Pomeron Exchange (DPE), the central system contains remnants from the diffractive exchange in addition to the hard subprocess.

## 2 Low Luminosity Running

At low luminosity, the diffractive processes can be detected using rapidity gaps. A possible L1 trigger would be based on a requirement of a rapidity gap on one or both sides from the IP and an activity in the central detector with energy over a certain threshold. The gap may span the region from the forward calorimeters of the ATLAS detector [2] or CMS detector [3] over the luminosity detectors (LUCID [4] in ATLAS or TOTEM [5] in CMS) up to ZDC detectors in ATLAS [6] or in CMS [3]. Measurements which would be straightforward and hence suitable for analyses of the very early LHC data are ratios of the kind of X+gaps/X(incl.), where X may be W, Z, dijet, heavy quark and dilepton, and X(incl.) means measuring X without requiring rapidity gaps. Measurements of ratios are convenient since many sources of systematic uncertainties are cancelled, particularly that of the luminosity at the early phase and among other, they also serve as valuable checks of different components of the formalism used to predict the CEP cross section by the KMR group [7, 8]. The soft survival probability,  $S^2$ , can be studied in electroweak processes, such as W+gaps or Z+ gaps.  $S^2$  is defined as a probability that additional soft secondaries will not populate the gaps and it explains the factorisation breaking observed at hadron colliders when diffractive parton density functions (dPDF) obtained in Single Diffraction (SD) at HERA were applied in measurements of SD by CDF [9]. The generalised gluon distribution,  $f_g$ , can be probed in exclusive  $\Upsilon$  production proceeding via either a photon

or an odderon exchange. The higher-order QCD effects, especially Sudakov-like factors and also a possible role of the enhanced absorptive corrections can be studied in exclusive two- or three-jet events. When the proton tagging becomes available, the  $t$ -dependence of the elastic, SD and DPE cross sections can be obtained and hence effect of individual components of the pile-up background can be evaluated.

## 2.1 Dijet Production in DPE and CEP

Without proton tagging, the dijet production in DPE and CEP can be measured by requiring two central jets and rapidity gaps on both sides of the IP in forward calorimeter, LUCID/TOTEM and ZDC. In DPE, the rapidity gaps may be spoiled by particles from the pomeron remnants and although the cross section is about two orders of magnitude larger than the CEP cross section at the same dijet mass, the CEP cross section will dominate if the forward calorimeter is required to be devoid of activity. The measurement of the dijet production in CEP at 7–14 TeV may be compared with a similar measurement made at Tevatron from which models used to describe the data may be constrained.

## 2.2 Gaps between Jets

By selecting events with two jets each in opposite side of forward calorimeter and a rapidity gap in the central detector, ATLAS and CMS can improve an existing measurement of this type by D0 [10] at centre-of-mass (c.m.s.) energy of 1.8 TeV. Different colour singlet exchange models can be tested by comparing data with predictions for the gap fractions as functions of rapidity between the jets.

# 3 High Luminosity Running

A great attention is recently devoted to the possibility of complementing the standard LHC physics menu by adding forward proton detectors (FPD) to the ATLAS and CMS detectors. They would detect a great part of the energy flow that escapes undetected by the main detectors.

## 3.1 SM and BSM Higgs Boson Production

The forward proton tagging will provide an exceptionally clean environment to search for new phenomena at the LHC and to identify their nature. Of particular interest in this context is the CEP which gives access to the generalised (or skewed) PDFs. The CEP of a SM (or MSSM) Higgs boson is attractive for two reasons: firstly, if the outgoing protons remain intact and scatter through small angles then, to a good approximation, the central system  $\phi$  must be produced in a  $J_z = 0$ , CP even state, therefore allowing a clean determination of the quantum numbers of any observed resonance. Here  $J_z$  is the projection of the total angular momentum along the proton beam axis. Secondly, from precise measurements of proton momentum losses,  $\xi_1$  and  $\xi_2$ , the mass of the central system can be measured much more precisely than from the dijet mass measured in the calorimeters, by the so-called missing mass method,  $M^2 = \xi_1 \xi_2 s$ , which is independent of the decay mode. The simplest decay mode from an experimental perspective is the WW decay mode, in which one (or both) of the W bosons decay leptonically. With standard single and double lepton trigger thresholds at ATLAS (or CMS), approximately 6 events are expected for Higgs boson mass around 160 GeV with luminosity of  $30 \text{ fb}^{-1}$  [11]. In

the  $b\bar{b}$  decay mode, the quantum number selection rules in CEP strongly suppress the QCD b-jet background, nevertheless severe requirements necessary to get rid of the pile-up background make the event yield rather modest [12, 13]. Full details of the calculation of the background to this channel are described in [14, 15].

In certain regions of the MSSM parameter space the cross section for the CEP of Higgs bosons is significantly enhanced and hence making the  $b\bar{b}$  decay mode attractive [15, 16]. In Fig. 1 an example mass spectrum is shown for MSSM Higgs boson candidates of mass of 120 GeV decaying into  $b\bar{b}$  for  $\tan\beta = 40$  (corresponding to the final cross section of about 18 fb) after 3 years of data taking at luminosity of  $2 \cdot 10^{33} \text{ cm}^{-2}\text{s}^{-1}$  or 3 years at  $10^{34} \text{ cm}^{-2}\text{s}^{-1}$ . At the low luminosity, the pile-up background can be completely eliminated and the statistical significance is around  $3.5\sigma$ . At the highest luminosity, fast timing detectors are necessary to reduce the pile-up background - significance of  $5\sigma$  is achieved with time resolution of 2 ps (see Section 4.4).

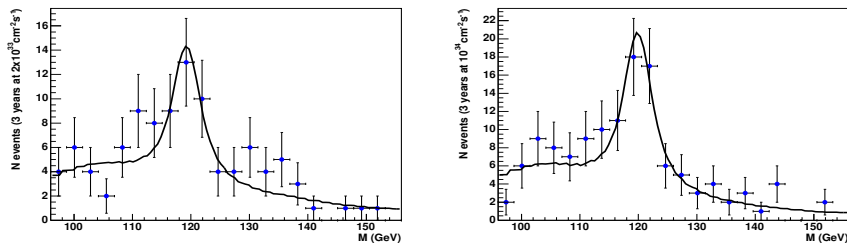


Figure 1: A typical mass fit of the  $H \rightarrow b\bar{b}$  signal and its backgrounds for 3 years of data taking with ATLAS and the 420+420 detector configuration (a) at  $2 \cdot 10^{33} \text{ cm}^{-2}\text{s}^{-1}$  ( $60 \text{ fb}^{-1}$ ). The significance of the fit is  $3.5\sigma$ . (b) at  $10^{34} \text{ cm}^{-2}\text{s}^{-1}$  after removing the pile-up background completely. The significance is  $5\sigma$ . Figures from [16].

### 3.2 Central Exclusive Jet Production

The tagging of both protons in FPDs will enable a measurement of the proton transverse momenta and azimuthal angles which allows us to study the opacity of the incoming protons, and more generally, to test the dynamics of the soft survival probability by studying the correlations between the outgoing protons [7, 17]. This can be carried out with the CEP of dijets as the cross section is large. Thanks to the  $J_z = 0$  selection rule which is applicable to all CEP processes, quark jet production is suppressed and the CEP can then be recognised as reduced ratio of b-jets to all jets when compared to other production processes.

### 3.3 Diffraction and QCD

The SD and DPE processes serve to provide an information about the low-x structure of the proton and the dPDFs. Inclusive jet and heavy quark production are mainly sensitive to the gluon component of the dPDFs, while vector boson production is sensitive to quarks. The kinematic region covered expands that explored at HERA and Tevatron, with values of  $\beta$  (the fractional momentum of the struck parton in the diffractive exchange) as low as  $10^{-4}$  and of  $Q^2$  up to  $10^4 \text{ GeV}^2$ . More information about the SD dijet and W boson production can be found elsewhere in these proceedings (V. Juranek and W. Carvalho)

## 3.4 Photon-Photon Physics

As the LHC beams act also as a source of high-energy photons a rich program of photon-photon and photon-proton physics can be pursued. Photon-induced processes have been extensively studied at LEP and HERA. However at LHC, these processes can be investigated in an unexplored region of the phase-space. The final state topology is similar to CEP, i.e. a central system, X, separated on each side by large rapidity gap from a very forward proton detected in the FPD. Different average proton transverse momenta make it possible to separate between diffractive and photon-induced events.

The W- and Z-pair production (as a tool to study anomalous triple and quartic gauge couplings) is discussed elsewhere in these proceedings (O. Kepka). The SUSY particle production is described by K. Piotrkowski in these proceedings and in [18].

### 3.4.1 Lepton Pair Production

Two-photon exclusive production of muon pairs has a well known QED cross section, including very small hadronic corrections [19]. Very recently, such event candidates have been observed by the CDF [20] and their cross sections found in a good agreement with theory. After applying simple selection criteria such as  $p_T > 10$  GeV,  $|\eta| < 2.5$  and requiring one forward proton tag, the cross section is 1.3 pb [1, 21]. This corresponds to approximately 50 muon pairs detected in a 12 hour run at a mean luminosity of  $10^{33}\text{cm}^{-2}\text{s}^{-1}$ . The large event rate coupled with a small theoretical uncertainty makes this process a perfect candidate for the absolute LHC luminosity calibration [22] and also of the FPD system at 420 m [1]. The  $e^+e^-$  production can also be studied, although the trigger thresholds will be larger and hence the final event rate reduced.

## 3.5 Photoproduction

The high luminosity and the high c.m.s. energies available for photoproduction processes at the LHC allows us to study electroweak interactions and to search Beyond the Standard Model up to the TeV scale [21].

### 3.5.1 Associated WH Production

As shown in [21], the cross section for the associated WH production ( $pp \rightarrow (\gamma p \rightarrow WHq') \rightarrow pWHq'Y$ ) after applying selection criteria and considering five different final states is 0.17 fb at  $m_H = 115$  GeV and 0.29 fb at  $m_H = 170$  GeV. The most promising channel seems to be the  $jjl^\pm l^\pm$  at  $m_H = 170$  GeV where the signal to irreducible background ratio is 0.22 fb/0.28 fb, so luminosity of  $100\text{fb}^{-1}$  might reveal the  $HWW$  gauge coupling.

### 3.5.2 Single Top Quark and Anomalous Top Quark Production

Photoproduction of single top quark ( $pp \rightarrow (\gamma p \rightarrow Wt) \rightarrow pWtY$ ) is dominated by t-channel amplitudes in association with a W boson which all are proportional to the CKM matrix element  $|V_{tb}|$ . The ratio of associated Wt production cross section to the sum of all top production cross sections is 5% for parton-parton interactions, while it is 50% in photoproduction. In [21] two topologies were studied, namely  $lbjj$  and  $llb$ . The signal cross section after selection cuts of about 44 fb with a signal to irreducible background ratio of 0.6 suggest that this mechanism and hence  $|V_{tb}|$  may be easily measurable even with luminosity of  $1\text{fb}^{-1}$ .

At LHC the exclusive single top quark photoproduction can only occur via flavour changing neutral current processes which are not present at tree level of SM but appear in many extensions of SM such as two Higgs-doublet models or R-parity violating supersymmetry. The final state of this  $pp \rightarrow (\gamma p \rightarrow t) \rightarrow ptY$  process is composed of a b-jet and a W boson. In [21] the leptonic  $lb$  topology was studied and only photoproduction  $\gamma p \rightarrow W + jet$  background considered. With an integrated luminosity of  $1 \text{ fb}^{-1}$  the expected limits for anomalous couplings  $k_{tu\gamma}$  and  $k_{tc\gamma}$  at 95% CL are greatly improved with respect to existing best estimates.

### 3.5.3 Photoproduction of Jets

In photoproduction of jets, the fraction of the photon,  $x_\gamma$ , and proton,  $x_p$ , four-momentum carried by a parton involved in binary hard scattering is calculated using the energies and angles of jets in the central detector and of the protons in the FPDs. The direct photon processes are characterised by  $x_\gamma \sim 1$  and resolved photon processes by  $x_\gamma < 1$ . The H1 and ZEUS collaborations have constrained the region  $x_p, x_\gamma > 0.1$  for diffractive photoproduction. At LHC we expect to reach values of  $x_p$  and  $x_\gamma$  of an order of magnitude lower than at HERA. Furthermore, the diffractive photoproduction of dijet systems at the LHC promises to shed light on the issue of the QCD factorisation breaking recently reported in the same process by the H1 experiment [23].

### 3.5.4 Exclusive $\Upsilon$ Production

Exclusive  $\Upsilon$  photoproduction,  $\gamma p \rightarrow \Upsilon p$  can be studied using FPDs [8], although only one proton can be tagged due to the low mass of the  $\Upsilon$ . The cross section is expected to be approximately 1.25 pb for the decay channel  $\Upsilon \rightarrow \mu^+ \mu^-$  and is sensitive to the same skewed unintegrated gluon densities of the proton as the CEP of Higgs boson. Measuring this process thus helps to constrain the  $f_g$  as the soft survival factor is expected to be close to 1. The  $\gamma p \rightarrow \Upsilon p$  process can also occur via odderon exchange and this channel could be the first evidence for the odderon's existence.

## 4 Future Forward Proton Upgrades at the LHC

The forward detectors and possible upgrades at ATLAS and CMS have been described elsewhere by A. Zoccoli in these proceedings.

### 4.1 FP420

The FP420 R&D collaboration [1], with members from ATLAS, CMS and LHC studied the possibility of installing high precision tracking and timing detectors at 420 m from the IP. Detection of the protons will be achieved by two 3D silicon detector stations at each end of the FP420 region. This novel technique provides high radiation-resistive detectors close to the beam with an insensitive area as small as  $5 \mu\text{m}$  and with a resolution of about  $15 \mu\text{m}$ . The tracking and timing detectors will be attached to a movable beam pipe. As the beam pipes in the 420 m region are contained in an interconnecting cryostat and the sensitive detectors are best operated at room temperature, a new connection cryostat has been designed using a modified Arc Termination Module at each end.

## 4.2 Coverage of the Region of 220–240 m

Both ATLAS and CMS collaborations work on equipping the region of 220 m (ATLAS) or 240 m (CMS) by FPDs. The proposed equipment would be very similar to that at 420 m; differences are mainly in no need to change the cryostat and in an addition of a detector to be used for L1 trigger. In ATLAS, the combined effort to install FPDs at 220 and 420 m led in the AFP project (ATLAS Forward Proton) [24].

## 4.3 Acceptance and Resolution

With the position resolution of  $15 \mu\text{m}$  we expect a mass resolution of the order of 1–2% for the 420+420 and about 3% for the 420+220 configurations over a mass range of 120–200 GeV. For given dipole apertures and collimator settings and a thin window of  $200 \mu\text{m}$ , the expected  $\xi$  range is 0.002–0.02 for 420+420 and 0.01–0.15 for the 420+220 configuration.

The low- $\xi$  (and therefore low mass) acceptance depends critically on the distance of approach of the active area of the sensitive detectors from the beam. The final distance of approach will depend on the beam conditions, machine-induced backgrounds and collimator positions, and the RF impact of the detector on the beams. At 420 m the nominal operating position is assumed to be between 5 and 7.5 mm, at 220 m it is between 2.0 and 2.5 mm. For masses above about 120 GeV, the 220 m detector adds to the acceptance with increasing importance as the central mass increases. The differences between ATLAS and CMS acceptances for the 420+420 as well as 420+220 configurations (see Fig. 2) are due to a different crossing angle which is in the vertical plane for IP1 (ATLAS) and horizontal plane at IP5 (CMS).

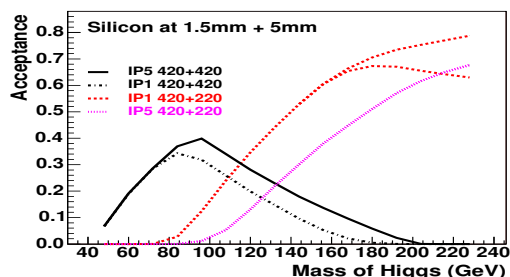


Figure 2: Mass acceptance for the 420+420 and 420+220 detector configurations (5 mm from the beam for 420 m and 1.5 mm for 220 m detectors) for IP1 and IP5. From [1].

## 4.4 Timing Detectors

The most prominent background to many diffractive physics analyses comes from an overlap of two soft SD events from pile-up and one ND event produced at a hard scale. Fast timing detectors with an expected sub-10 ps time resolution corresponding to a vertex resolution of better than 2.1 mm should be able to assign a vertex to the proton detected in the FPD and to reject about 97% of cases that appear to be CEP events but where the protons in reality originated from coincidences with pile-up events. Presently two detector options are studied, namely Quartz and Gas Cerenkov which may be read out with a Constant Fraction Discriminator allowing the time resolution to be significantly improved compared to usual electronics.

## 4.5 Trigger

Due to a limited L1 trigger latency, detectors at 420 m are far away from the central detectors to be included in the L1 trigger in normal running conditions, while detectors at 220 m can in principle be included. The trigger strategy depends on the mass of the diffractively produced object [12]. Demanding standard L1 triggers such as those for high mass  $H \rightarrow WW/ZZ$  or high- $p_T$  dijet trigger would result in an acceptable output rate which may be further reduced by requiring the double proton tag at 220 m.

Triggering on low mass objects is more difficult but in principle feasible as documented in [25, 26] where diffractive L1 triggers for a case of  $H \rightarrow b\bar{b}$  at  $m_H=120$  GeV have been proposed. If the FPD trigger at 220 m is capable of triggering only on hits in the inner 4 mm part and if the L1 calorimeter is capable of defining exclusivity criteria using  $E_T, \eta$  and  $\phi$ , then the final output rate is well below a 2 kHz limit at  $\mathcal{L} = 2 \cdot 10^{33} \text{cm}^{-2} \text{s}^{-1}$  and slightly above this limit at  $\mathcal{L} = 10^{34} \text{cm}^{-2} \text{s}^{-1}$ . Other reductions are under study [26].

## Acknowledgements

Supported by the project AV0-Z10100502 of the Academy of Sciences of the Czech republic and project LC527 of the Ministry of Education of the Czech republic.

## References

- [1] FP420 R&D Collab., J. Inst.: 2009-JINST-4-T10001, arXiv:0806.0302 [hep-ex].
- [2] ATLAS Collab., J. Inst. 0803: S08003 (2008).
- [3] CMS Collab., J. Inst. 0803: S08004 (2008).
- [4] ATLAS Collab., CERN-LHCC-2004-010 (2004); A. Zoccoli, these proceedings.
- [5] TOTEM Collab., CERN-LHCC-2004-002 (2004); S. Giani, these proceedings.
- [6] ATLAS Collab., CERN-LHCC-2007-001 (2007).
- [7] V. A. Khoze, A. D. Martin and M. G. Ryskin, Eur. Phys. J. **C 23** (2002) 311.
- [8] V. A. Khoze, A. D. Martin and M. G. Ryskin, arXiv:0802.0177 [hep-ph].
- [9] CDF Collab., Phys. Rev. Lett. **84** (2000) 5043.
- [10] D0 Collab., Phys. Lett. **B440** (1998) 189.
- [11] B. E. Cox *et al.*, Eur. Phys. J. **C45** (2006) 401.
- [12] M. Albrow *et al.*, CERN-LHCC-2006-039 (2006).
- [13] A. Brandt, V. Juránek, A. Pal and M. Taševský, Atlas note in preparation.
- [14] V. Khoze *et al.*, Eur.Phys.J.**C25** (2002) 392; A.G. Shuvaev *et al.*, Eur.Phys.J.**C56** (2008) 467.
- [15] S. Heinemeyer *et al.*, Eur.Phys.J.**C53** (2008) 231.
- [16] B.E. Cox, F.K. Loebinger, A.D. Pilkington, JHEP 0710:090 (2007).
- [17] CDF Collab., arXiv:0712.0604 [hep-ex].
- [18] K. Piotrkowski and N. Schul, arXiv:0806.1097 [hep-ph].
- [19] V. A. Khoze, A. D. Martin, R. Orava and M. G. Ryskin, Eur. Phys. J. **C 19** (2001) 313.
- [20] CDF Collab., Phys. Rev. Lett. **98** (2007) 112001; M. Albrow, these proceedings.
- [21] J. Favereau de Jeneret *et al.*, CP3-09-37 (August 2009), arXiv:0908.2020 [hep-ph].
- [22] K. Piotrkowski, Phys. Rev. **D63** (2001) 071502.
- [23] H1 Collab., Eur. Phys. J. **C 51** (2007) 549.
- [24] ATLAS Collab., Letter of Intent of the AFP project.
- [25] M. Grothe *et al.*, CERN-CMS-NOTE-2006-054.
- [26] M. Campanelli *et al.*, ATLAS-COM-DAQ-2009-062.